Mechanical Engineering Faculty Publications   Mechanical Engineering Department

2002

Comparison of Mobility Method and Mass Conservation Method in a Study of Dynamically Loaded Journal Bearings

Biao Yu
Cleveland State University

Jerzy T. Sawicki
Cleveland State University, j.sawicki@csuohio.edu

Comparison of Mobility Method and Mass Conservation Method in a Study of Dynamically Loaded Journal Bearings

BIAO YU and JERZY T. SAWICKI*

Fenn College of Engineering, Rotor-Bearing Dynamics and Diagnostics Laboratory, Cleveland State University, Cleveland, Ohio 44115-2425, USA

The inverse problem of dynamically loaded journal bearings was solved using generalized Reynolds equation coupled with a complete mass conservative cavitation boundary conditions, as outlined by the Jacobsson-Floberg and Olsson (JFO) cavitation theory. In the course of solution, the modified Thomas algorithms was employed, instead of standard Gauss–Jordan reduction method, which fully utilizes the sparse character of the system matrix, and thus greatly reduces computational time. The developed model was tested against the well-known mobility method for the case of journal bearings in a commercial reciprocating air compressor. It was found that the mobility method overestimates minimum film thickness and underestimates such parameters as lubricant flow rate and bearing power loss. In general, the level of error is acceptable for most industrial applications. However, for the journal bearing where the feed pressure is time dependent and starvation effects are predominant, the mobility method may produce large not acceptable errors.

The performance of dynamically loaded bearings is an important issue for the engine industry. Recently, two approaches may be observed in the course of the development of bearing design and analysis. On the one hand, there is a need in industry for a quick method or algorithm for engineers who desire to have a reliable and rapid design tool. On the other hand, the more involved applications drive researchers to explore lubrication phenomena in a comprehensive depth, using very complex mathematical methods, with a hope to solve a more realistic bearing problem.

For a finite journal bearing, which lubrication behavior can be described by 2D Reynolds equation, there does not exist analytical solution. The analytical solutions are possible to obtain only for some specific bearing configurations (Anaya-Dufresne et al., 1995). However, for a non-ideal, finite length bearing, numerical method has to be applied.

Cavitation is inevitable for submerged journal bearings, like in a case of journal bearing system in most of reciprocating machinery. The purpose of early cavitation theories was to predict the boundaries between the full fluid film and the gas region through some simple assumptions. Then, the Reynolds equation can still be applied in the full fluid film regions. Sommerfeld (1904) assumed that non-cavitating boundary conditions are fixed at film angles $0°$ and 2π, respectively, which obviously violates mass conservation principle and is even not true for a steadily loaded bearing. Gumbel (1914) suggested another boundary conditions, which set all predicted negative pressures by the Reynolds equation to the cavitation pressure (Gumbel boundary condition). Although the Gumbel boundary condition produces reasonable load values, the assumption still violates the conservation principle of mass, thus produces poor approximate values of flow rate and power loss. A better cavitation boundary condition was first suggested by Swift (1932) and Stieber (1933), which is called Reynolds boundary condition in the literature. In this type of boundary condition, the film pressure is assumed to develop from the point of maximum film thickness to the location where the pressure gradient vanishes. Here, the film rupture is appropriately treated in the mass conservation sense, but the film reformation is kept under the same assumption as that in Sommerfeld boundary condition. Therefore, the Reynolds boundary condition is not a complete mass conservative boundary

condition. For a dynamically loaded bearing with partial groove, the flow rate predicted by Reynolds boundary condition can be higher by as much as 100% or more than that measured from experiments (Etsion et al., 1975). Finally, Floberg (1957); Jakobsson and Floberg (1957) and Olsson (1965) formulated a complete mass conservative boundary condition for a moving boundary that ensured mass flow continuity at film rupture as well as at film reformation (JFO boundary conditions).

Unfortunately, JFO boundary conditions turned out to be quite difficult for computer programming, because boundaries of rupture and reformation, which change with the transient load, have to be traced all the time. Therefore, JFO boundary conditions were not widely used until Elrod (1981) suggested to overcome the bookkeeping task by introducing a so called later Elrod algorithm, which automatically conforms the requirements of mass conservation and the JFO boundaries. Using this algorithm, Brewe (1986) and Woods and Brewe (1989) calculated dynamically loaded journal bearing and found excellent agreement with Jakobsson's experimental data (Jakobsson et al., 1957). Next, Vijayaghavan (1989) extended the Elrod's method by discretizing a universal Reynolds equation directly. Since the Vijayaghavan algorithm exhibits better handling of lubricant compressibility effects than Elrod algorithm, it has been chosen for the modeling of the bearing lubrication, and it will be called the *rigorous method* by the authors in this study.

With the solution of Reynolds equation, pressure distributions can be calculated if eccentricity of bearing journal center is specified. Then the fluid film supported load can be obtained from the integration of the pressure distributions. This is so-called a direct problem. However, for journal bearings in reciprocating machinery, usually the inverse problem needs to be solved, i.e., dynamical loads on bearing are known but eccentricities of journal need to be sought. The inverse problem is more difficult to solve than the direct problem, because it has to be solved through an iterative fashion, which makes the analysis more complex and time-consuming. There have been some attempts to quickly predict the journal center trajectory during the load cycle range. Booker (1965) suggested so-called mobility method. He defined the velocity vector of a journal bearing center as a function of its load and position vectors, and derived mobility vectors, which define the pure squeeze velocity vector in terms of the load and position vectors. The mobility method enables a full orbit of journal center to be calculated very rapidly, without reiterative calculations at each time step. However, the method has a number of limitations, which make it not appropriate in the analysis of the following cases:

- The bearing is not fully flooded by the lubricant (starvation effects).
- The viscosity of lubricant is pressure dependent (compressibility effects).

- The bearing is partially grooved in circumferential direction (non-circumferential symmetrical effects).

Furthermore, the mobility method employs Gumbel boundary condition for cavitation, which is not mass conservative and therefore it may generate significant error.

The purpose of this paper is to compare the results produced by the mobility method and the rigorous method, while both are applied for the analysis of dynamically loaded bearings in a commercially available reciprocating air compressor.

FORMULATION AND PROCEDURE

Governing Equations

Reynolds Equation

The fluid movement within the bearing can be simplified as a two-dimensional, compressible, unsteady, viscous flow

$$\frac{\partial \rho h}{\partial t} + \frac{\partial}{\partial x}\left[\frac{\rho h(u_j + u_b)}{2}\right] - \frac{\partial}{\partial x}\left(\frac{\rho h^3}{12\mu}\frac{\partial p}{\partial x}\right)$$
$$- \frac{\partial}{\partial y}\left(\frac{\rho h^3}{12\mu}\frac{\partial p}{\partial y}\right) = 0 \tag{1}$$

with the corresponding axial boundary conditions

$$p(\theta, \pm L/2) = 0 \tag{2}$$

Universal Reynolds Equation

According to Elrod and Adams (1975), the universal Reynolds Equation, which is not only valid in a full film region but also in a cavitated zone, can be derived from Eq. [1] as

$$\frac{\partial(h\varphi)}{\partial t} + \frac{\partial}{\partial x}\left(\frac{hU\varphi}{2} - \frac{\beta h^3 g}{12\mu}\frac{\partial \varphi}{\partial x}\right)$$
$$+ \frac{\partial}{\partial y}\left(-\frac{\beta h^3 g}{12\mu}\frac{\partial \varphi}{\partial y}\right) = 0 \tag{3}$$

where:

$$\varphi = \begin{cases} \rho/\rho_c & \text{in full film regions} \\ V_f/V_c & \text{in cavitated regions} \end{cases} \tag{4}$$

$$g = \begin{cases} 1 & \text{when } \varphi \geq 1 \\ 0 & \text{when } \varphi < 1 \end{cases} \tag{5}$$

$$\beta = \rho\frac{\partial p}{\partial \rho} = \varphi\frac{\partial p}{\partial \varphi} \tag{6}$$

In the above equations, V_c and V_f are the total clearance volume and the volume occupied by the fluid, respectively, ρ_c is the fluid density within cavitated zone, g is the switch function, and β is the bulk modulus of the lubricant. One can integrate Eq. [6] to obtain

$$p = p_c + g\beta \ln \varphi \qquad [7]$$

Mobility Method

Booker (1965) rewrote Eq. [1] in polar coordinate system for isoviscous flow as

$$\frac{\partial}{\partial \theta}\left[(1 + \varepsilon \cos \theta)^3 \frac{\partial p}{\partial \theta}\right] + R^2 \frac{\partial}{\partial y}\left[(1 + \varepsilon \cos \theta)^3 \frac{\partial p}{\partial y}\right]$$
$$= 12\mu(R/C)^2[\dot{\varepsilon} \cos \theta + \varepsilon(\dot{\phi} - \overline{\omega}) \sin \theta] \qquad [8]$$

where $\overline{\omega}$ is the average angular velocity of journal and sleeve (bearing) relative to the load line, $\dot{\phi}$ is the load vector velocity relative to the line of centers, $\overline{\omega}$ is positive in CCW, whereas $\dot{\phi}$ is positive in CW, as shown in Figure 1.

Finally, Eq. [8] can be written to express a relationship between squeeze film speed and mobility vector as

$$\dot{\varepsilon} = \frac{F(C/R)^2}{\mu LD} \cdot M\left(\varepsilon, \frac{L}{D}\right) + \overline{\omega} \times \varepsilon \qquad [9]$$

If the mobility vector M, initial position vector ε and load F are known, it is easy to obtain ε in current time step from Eq. [9]. The mobility vector M for a finite bearing can be obtained using numerical calculation and curve fits, as demonstrated by Goenka (1984).
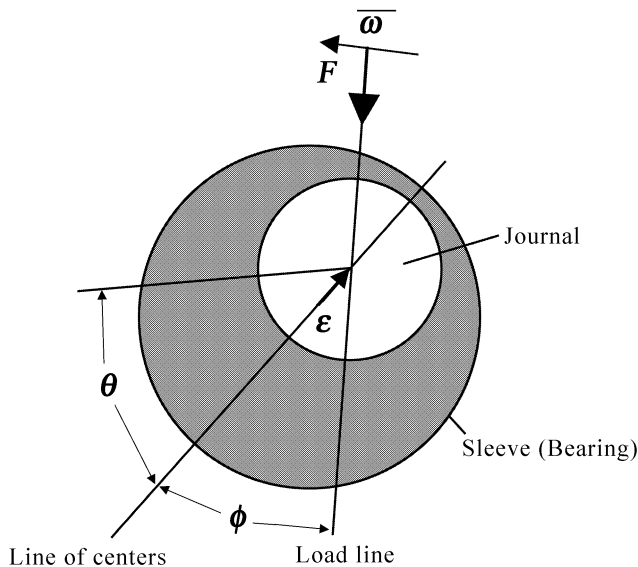

FIGURE 1 Film geometry for dynamically loaded bearing.

Load Capacity of Journal Bearing

The load supported by the bearing can be calculated through the following two integral equations in polar coordinates (Figure 1),

$$F_r = -R \int_{-L/2}^{L/2} \int_0^{2\pi} p \cos \theta \cdot d\theta \cdot dy$$
$$F_\theta = R \int_{-L/2}^{L/2} \int_0^{2\pi} p \sin \theta \cdot d\theta \cdot dy \qquad [10]$$

where F_r and F_θ are radial and circumferential load components, respectively. Next, Eq. [10] may be transformed into the $x-y$ coordinate frame as follows:

$$F_r = -F_x \cos \phi - F_y \sin \phi$$
$$F_\theta = -F_x \sin \phi + F_y \cos \phi \qquad [11]$$

Numerical Procedure

Universal Reynolds Equation

Equation [3] is discretized by finite difference scheme using Vijayaghavan's algorithm (1989), and for each node it takes the following form

$$b_i \varphi_{i-1}^{k+1} + d_i \varphi_i^{k+1} + a_i \varphi_{i+1}^{k+1} = c_i \quad i = 1, \ldots, m \qquad [12]$$

An alternating direction implicit (ADI) scheme developed by Douglas and Gunn (1955) which is second-order accurate in time and space, with a truncating error of $O[(\Delta t)^2, (\Delta x)^2]$, was employed to find the distribution of φ. The time step is split into two sub-steps. In the first half of time step the matrix is solved for each row (circumferential direction) of grid points, while in the second half the matrix is solved for each column (axial direction) of grid points. The switch function g is updated immediately after each half-time step, to avoid possible numerical oscillations (Brewe, 1986). For the second half of time step, all the boundary conditions are of Dirichlet type, and Eq. [12] can be expressed in matrix form as follows:

$$\begin{bmatrix} d_1 & a_1 & \cdot & & \cdot & 0 \\ b_2 & d_2 & a_2 & & \cdot & \cdot \\ \cdot & \cdot & \cdot & & \cdot & \cdot \\ \cdot & \cdot & b_{m-1} & d_{m-1} & a_{m-1} \\ 0 & \cdot & & \cdot & b_m & d_m \end{bmatrix} \begin{bmatrix} \varphi_1^{k+1} \\ \varphi_2^{k+1} \\ \cdot \\ \varphi_{m-1}^{k+1} \\ \varphi_m^{k+1} \end{bmatrix} = \begin{bmatrix} c_1 \\ c_2 \\ \cdot \\ c_{m-1} \\ c_m \end{bmatrix} \qquad [13]$$

Equation [13] presents a tridiagonal matrix system and can be solved by Thomas algorithm (Anderson et al., 1984). However, for the first half time step, some rows in circumferential direction do not meet any boundary points.

In that case, periodic or wrap-around boundary conditions should be applied as

$$\varphi(\theta + 2\pi) = \varphi(\theta) \qquad [14]$$

Now, Eq. [12] can be written in matrix format as:

$$\begin{bmatrix} d_1 & a_1 & \cdot & \cdot & b_1 \\ b_2 & d_2 & a_2 & \cdot & \cdot \\ \cdot & \cdot & \cdot & \cdot & \cdot \\ \cdot & \cdot & b_{m-1} & d_{m-1} & a_{m-1} \\ a_m & \cdot & \cdot & b_m & d_m \end{bmatrix} \begin{bmatrix} \varphi_1^{k+1} \\ \varphi_2^{k+1} \\ \cdot \\ \varphi_{m-1}^{k+1} \\ \varphi_m^{k+1} \end{bmatrix} = \begin{bmatrix} c_1 \\ c_2 \\ \cdot \\ c_{m-1} \\ c_m \end{bmatrix} \qquad [15]$$

Nevertheless, the matrix in Eq. [15] is not tridiagonal, due to the appearance of terms a_m and b_1 in the corners of the matrix. Therefore, the Thomas algorithm can not be used directly for the solution. Vijayaraghavan (1989) suggested lagging of the two off-diagonal terms to make matrix in Eq. [15] a tridiagonal one with applicable Thomas algorithm. Unfortunately, the lagging method is dubious when being used for dynamically loaded bearing case. Of course, there are many other robust methods to solve Eq. [15], for example, Brewe (1986) used Gauss–Jordan elimination method, but he found it to be very slow.

Modified Thomas Method

To solve the non-tridiagonal matrix system described by Eq. [15], a modified Thomas method was developed by the authors. The detailed development can be found in Yu (1999). Here, only brief steps will be demonstrated.

At first, the Thomas algorithm is used to remove b_i terms in the matrix of Eq. [15]. The initial successive steps are very similar to those in Thomas algorithm, i.e.,

$$d_i = d_i - \frac{b_i}{d_{i-1}} a_{i-1}$$

$$c_i = c_i - \frac{b_i}{d_{i-1}} c_{i-1}$$

$$e_i = \begin{cases} -(b_i/d_{i-1})e_{i-1}, & \text{if } i \neq m-1 \\ a_{m-1} - (b_i/d_{i-1})e_{i-1}, & \text{if } i = m-1 \end{cases}$$

where $i = 2, \ldots, m-1$ and $e_1 = b_1$.

In the above equations, the equality signs mean, "is replaced by", as in the computer programming language. Now Eq. [15] becomes

$$\begin{bmatrix} d_1 & a_1 & \cdot & \cdot & b_1 \\ 0 & d_2 & a_2 & \cdot & e_2 \\ \cdot & \cdot & \cdot & \cdot & \cdot \\ \cdot & \cdot & 0 & d_{m-1} & e_{m-1} \\ a_m & \cdot & \cdot & b_m & d_m \end{bmatrix} \begin{bmatrix} \varphi_1^{k+1} \\ \varphi_2^{k+1} \\ \cdot \\ \varphi_{m-1}^{k+1} \\ \varphi_m^{k+1} \end{bmatrix} = \begin{bmatrix} c_1 \\ c_2 \\ \cdot \\ c_{m-1} \\ c_m \end{bmatrix} \qquad [16]$$

Next, the task is to "move" the off-diagonal term in the last row, a_m, to the diagonal line. Assuming $A_1 = a_m$, then

$$A_i = \begin{cases} -(A_{i-1}/d_i)a_i, & \text{if } i \neq m-2 \\ b_m - (A_{i-1}/d_i)a_i, & \text{if } i = m-2 \end{cases}, \quad i = 2, \ldots, m-2$$

$$c_m = c_m - \frac{A_{i-1}}{d_i} c_i, \quad i = 2, \ldots, m-2$$

$$d_m = d_m - \frac{A_{i-1}}{d_i} e_i, \quad i = 2, \ldots, m-2$$

$$e_m = d_m - \frac{A_{m-2}}{d_{m-1}} e_{m-1}$$

$$c_m = c_m - \frac{A_{m-2}}{d_{m-1}} c_{m-1}$$

where $i = 2, \ldots, m-1$.

The final matrix system takes the form:

$$\begin{bmatrix} d_1 & a_1 & \cdot & \cdot & b_1 \\ 0 & d_2 & a_2 & \cdot & e_2 \\ \cdot & \cdot & \cdot & \cdot & \cdot \\ \cdot & \cdot & 0 & d_{m-1} & e_{m-1} \\ 0 & \cdot & \cdot & 0 & e_m \end{bmatrix} \begin{bmatrix} \varphi_1^{k+1} \\ \varphi_2^{k+1} \\ \cdot \\ \varphi_{m-1}^{k+1} \\ \varphi_m^{k+1} \end{bmatrix} = \begin{bmatrix} c_1 \\ c_2 \\ \cdot \\ c_{m-1} \\ c_m \end{bmatrix} \qquad [17]$$

The solutions of Eq. [17] are found as:

$$\varphi_m = \frac{c_m}{e_m}$$

$$\varphi_{m-1} = \frac{c_{m-1} - e_{m-1}\varphi_m}{d_{m-1}}$$

$$\varphi_i = \frac{c_i - a_i\varphi_{i+1} - e_i\varphi_m}{d_i}, \quad i = m-2, \ldots, 1$$

Table I shows a comparison of computational efficiency using different algorithms for the solution of Eq. [15]. The modified Thomas method has the same efficiency as the Vijayaraghavan's lagged method. However, only the former one is suitable for the dynamically loaded bearing case. Furthermore, to solve an inverse problem for dynamically loaded bearing, considering that it is necessary to solve Eq. [15] iteratively all the time, it is a significant

TABLE I Comparison of different algorithms

Method	Number of multiplications	Applicable to dynamically loaded bearing analysis
Thomas algorithm (Vijayaraghavan lagged method)	$\sim m$	No
Modified Thomas algorithm (by the authors)	$\sim m$	Yes
Gauss–Jordan elimination method	$\sim m^3$	Yes

saving of time if the modified Thomas algorithm completes the calculation.

Calculation Procedure

All the non-boundary nodes are assigned by the initial condition ($\varphi = 1$ and $g = 1$), and boundary nodes are specified through Eq. [7]. This initial condition assumes that the eccentricity ratio and the load capacity are zeros for the bearing at the starting time of the calculation. If the actual load is added in at this instant, a large numerical disturbance is introduced and numerical instability may occur. To avoid this to happen, first a gradually increasing quasi-load has been applied to the bearing. As the load increases gradually, the eccentricity ratio is increased until the direction and value of the quasi-load is equal to that of the actual load. Then the actual load replaces the quasi-load and a normal calculation cycle starts. This process is called "*run-in*" procedure.

At a given time step, the initial φ results from the last-step calculation, then a guessed eccentricity ratio ε is

TABLE II   Parameters of two bearings

Main bearing	Length	0.018288 m
	Radius	0.02743 m
	Groove length (circumferential direction)	0.0249 m
	Groove width (axial direction)	0.00381 m
	Radial clearance	4.89×10^{-5} m
Connecting rod bearing	Groove length (circumferential direction)	0.00762 m
	Groove width (axial direction)	0.00762 m
	Length	0.02235 m
	Radius	0.01445 m

chosen to calculate hydrodynamic pressure distribution in the bearing. The resultant load carrying capacity can be obtained through the integration over the pressure distribution. If the resultant load is equal to the load added to the bearing, then the code goes to next time step; if not, the value of guessed ε is changed and the calculation
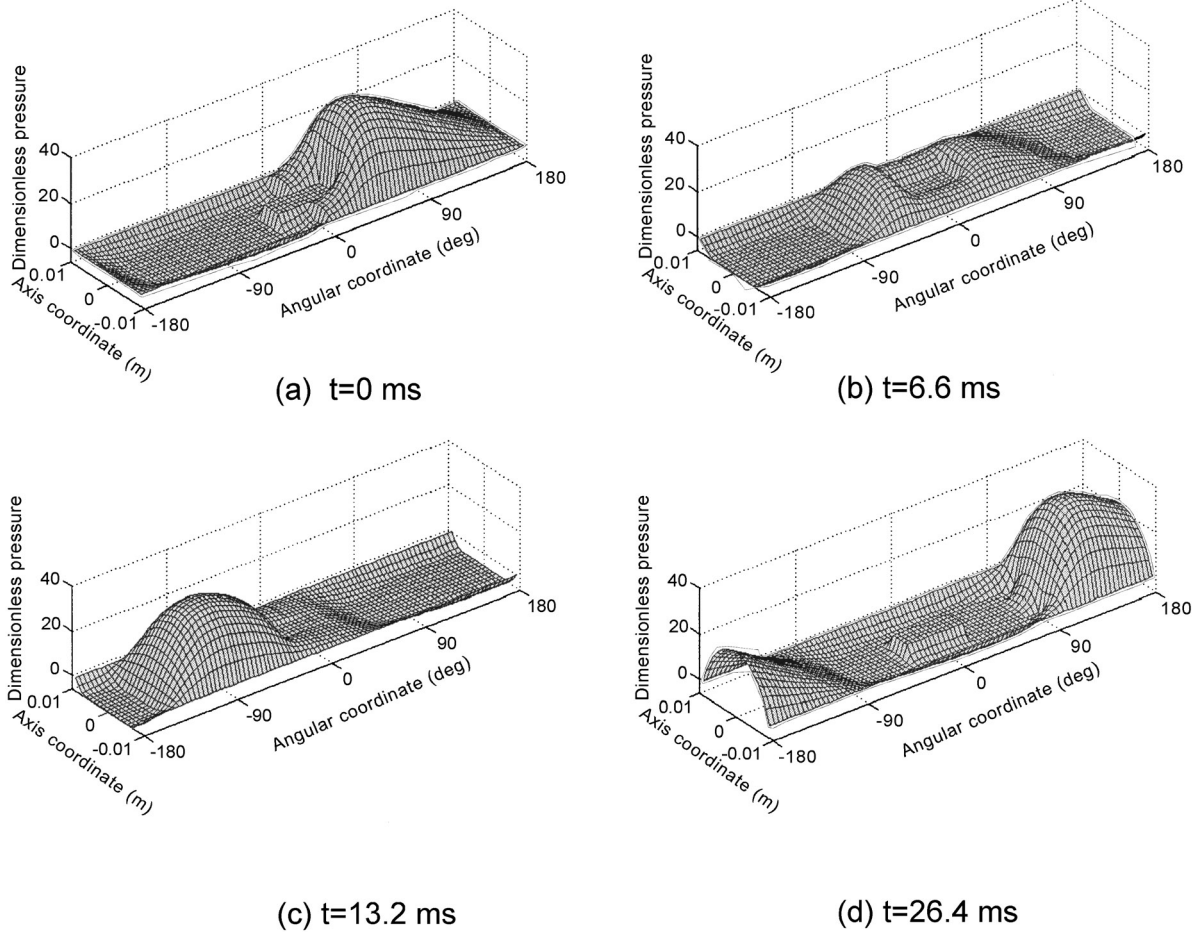

(a) t=0 ms

(b) t=6.6 ms

(c) t=13.2 ms

(d) t=26.4 ms

FIGURE 2   Pressure distribution in the main crankshaft bearing ($\omega = 1800$ rpm, $P_{feed} = 0.2068$ MPa).

(a) Load components

(b) Feed pressure

(c) Eccentricity ratio

(d) Minimum film thickness
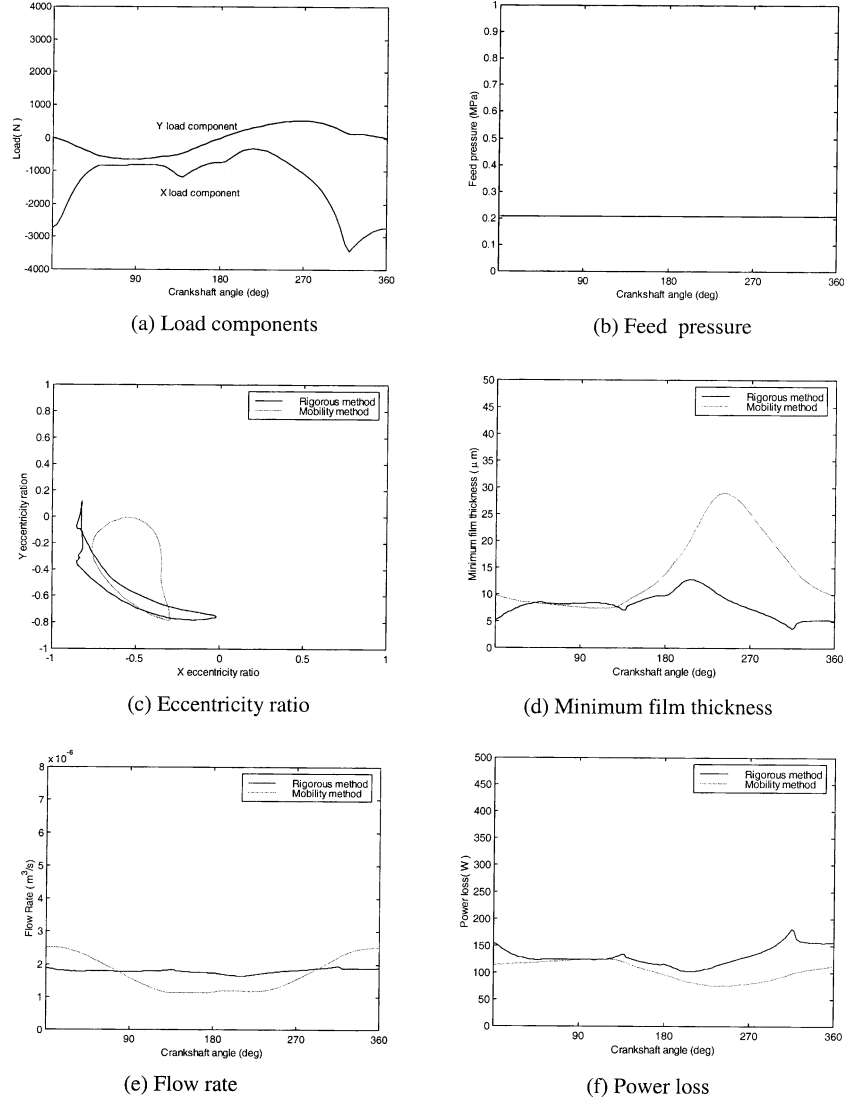

(e) Flow rate

(f) Power loss

FIGURE 3   Results for main crankshaft bearing ($\omega = 1800$ rpm, $P_{\text{feed}} = 0.2068$ MPa).

repeats again by keeping the same time step. This procedure is terminated when the periodic condition is satisfied, i.e., $|\varphi(t) - \varphi(t+\tau)| < \varepsilon$ where τ is the time required to complete one duty cycle by the machine, and ε is the convergence tolerance. In other words, we do not consider the solution as a convergent one until φ repeats itself in the cycle.

Formulas for calculation of power loss and flow rate may be found in a book of Pinkus and Sternlicht (1961).

RESULTS AND DISCUSSION

A main crankshaft bearing and a connecting rod bearing of a commercially available reciprocating air compressor have

been selected for this case study (Table II). Each bearing has partial circumferential groove. Cycling load on each bearing is shown in Figure 3(a) and Figure 4(a), respectively. The main bearing has constant lubricant feed pressure (Figure 3(b)), whereas the connecting rod bearing has time dependent lubricant feed pressure (Figure 4(b)).

Figure 2 shows that the cavitation bubble and the pressure peak are moving circumferentially (crankshaft speed = 1800 rpm, feed pressure = 0.2068 MPa) in the main bearing. Especially, when the pressure peak crosses the groove, the profile of pressure peak is much distorted (Figure 2(b)). The load capacity and other performance parameters of the bearing may be impacted due to the groove. For steady load acting on bearing, it is not difficult to find a suitable groove position to avoid the loss of load
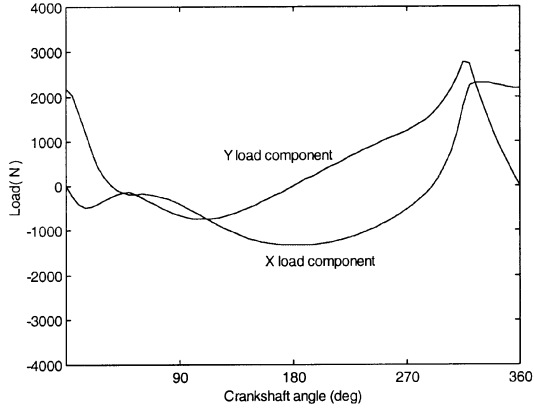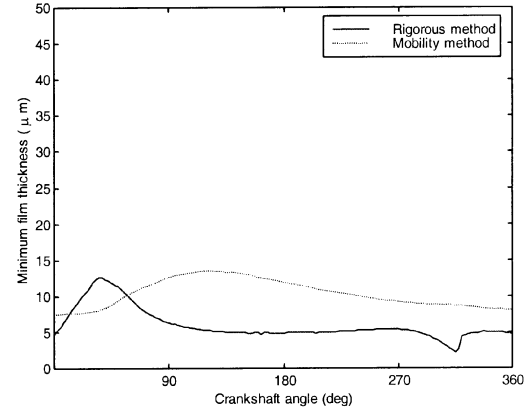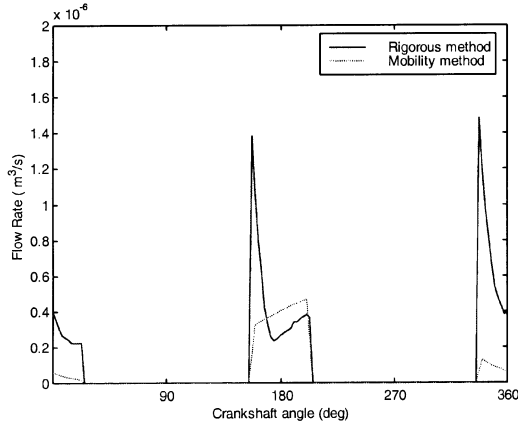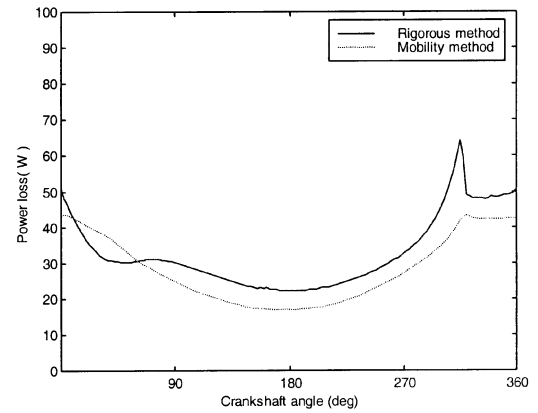
(a) Load components
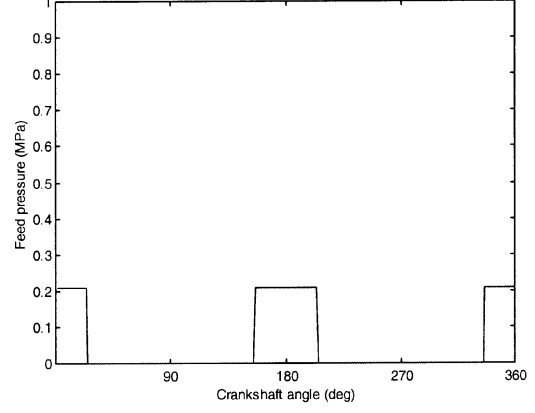
(b) Feed pressure
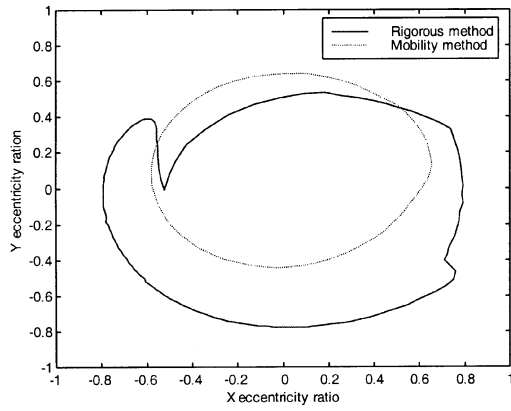
(c) Eccentricity ratio

(d) Minimum film thickness

(e) Flow rate

(f) Power loss

FIGURE 4   Results for connecting rod bearing ($\omega = 1800$ rpm, $P_{feed} = 0.2068$ MPa, $\varphi = 0.01$).

capacity. In the case of dynamical load, the loss can not be avoided, however, the position of the groove can be optimized so that the weakening of the load capacity would be minimized. Figures 3(c)–3(f) demonstrate the

calculation results for the main bearing. Generally, both approaches produce similar results. The maximum cycle averaged deviation predicted by these totally different methods is less than 25%, although the deviation in the

minimum film thickness is much higher. These results demonstrate that the mobility method, though based on a simple physical model, does depict well the main lubrication mechanisms in a fully flooded bearing. It generates reasonable and reliable estimation in the bearing design process as a rapid approach. So, it is no unusual to find that many automotive manufacturers still use the mobility method as their routine design tool. For example, in a Pentium 266 PC, the typical time needed by the mobility method to finish one cycle is about 10 seconds. However, it takes 20–30 hours to complete the same task if the rigorous method is applied.

However, the mobility method often underestimates cycle average eccentricity ratio, cycle average flow rate, cycle average power loss, and overestimates minimum film thickness in comparison to the rigorous method. In other words, if a bearing designer employs the mobility method for the design, it is recommended to choose a larger safety factor for the minimum film thickness, the power loss and the lubricant pump capacity.

In opposite to the main bearing, which always enjoys constant lubricant feed pressure and therefore has fully flooded lubrication conditions, the connecting rod bearing encounters conditions of starved lubrication. Figures 4(c) – 4(f) present the calculation results for this bearing. It is found that the mobility method generates larger deviation from the rigorous method than in the case of the main bearing, especially in estimating the amount of flow rate (the difference is more than 70%). This is the result of simple cavitation model and the assumption of constant feed pressure in the mobility method.

CONCLUDING REMARKS

Mobility method is a very efficient tool to obtain a quick solution in a process of dynamically loaded journal bearing design. For the constant feed pressure bearings, such as the main crankshaft bearing in the considered reciprocating compressor, it provides quite good results. The deviation compared to the rigorous method is less than 25%. In general, this level of error is acceptable for a bearing designer. However, quite significant error may be generated when the mobility method is employed for the analysis of connecting rod bearings, which have the characteristics of time dependent feed pressure. The deviation of cycle value may be even greater than 70%, when compared to the more accurate solutions.

NOMENCLATURE

C radial clearance of bearing, m
D diameter of bearing, m

F_x dynamical force in x-direction (laboratory coordinate), N
F_y dynamical force in y-direction (laboratory coordinate), N
F_ϕ dynamical force in film coordinate, N
F_r dynamical force in radial direction, N
g switch function, non-dimensional
h lubricant film thickness, m
L width of bearing, m
M mobility vector of bearing, nondimensional
p pressure, Pa
P_{feed} feed pressure of bearing, Pa
p_0 dimensionless pressure, $p(\Delta R)^2/R^2\mu\omega$
p_c pressure within cavitated zone, Pa
R radius of bearing, m
t time, s
u_j journal velocity, m/s
u_b bearing velocity, m/s
V_c total cavitated volume in cavitation area, m^3
V_f fluid volume in cavitation area, m^3
β lubricant bulk modulus, N/m^2
μ lubricant viscosity, Pa·s
ϕ angular coordinate along circumference relative to center line, rad
φ fractional film content in cavitated zone or density ratio in full film zone, non-dimensional
ρ lubricant density, kg/m^3
ρ_c lubricant density within cavitated zone, kg/m^3
τ machine cycle time, s
ω angular velocity of shaft, rpm or rad/s
$\bar{\omega}$ average angular velocity of journal and bearing relate to load line, rad/s
ε eccentricity ratio of bearing, or calculation error limit, non-dimensional

REFERENCES

Anaya-Duffresne, M. and Sinclair, G. B. (1995) Some Exact Solutions of Reynolds Equation, *ASME Journal of Tribology*, **117**, 560–562.
Anderson, D. A., Tannehill, J. C. and Pletcher, R. H. (1984) *Computational Fluid Mechanics and Heat Transfer*, McGraw-Hill Book Company.
Booker, J. F. (1965) Dynamically Loaded Journal Bearings: Mobility Method of Solution, *Journal of Basic Engineering*, Series D, **87**(3), 537–546.
Brewe, D. E. (1986) Theoretical Modeling of the Vapor Cavitation in Dynamically Loaded Journal Bearings, *ASME Journal of Tribology*, **108**, 628–638.
Douglas, J. Jr. and Gunn, J. E. (1964) A General Formulation of Alternating Direction Methods, Part I. Parabolic and Hyperbolic Problems, *Numerische Mathematik*, **6**, 428–453.
Elrod, H. G. and Adams, M. L. (1975) A Computer Program for Cavitation and Starvation Problems, *Cavitation and Related Phenomena in Lubrication*, Dowson, D., Godet, M. and Taylor, C. M. Eds., Mechanical Engineering Publications, New York, pp. 37–41.
Elrod, H. G. (1981) A Cavitation Algorithm, *Journal of Lubrication Technology*, **103**(3), 350–354.

Etsion, I. and Pinkus, O. (1975) Solution of Finite Journal Bearings with Incomplete Films, *Journal of Lubrication Technology*, **97**, 89–100.

Floberg, L. (1957) The Infinite Journal Bearing, Considering Vaporization, *Chalmers Tekniska Hogskolas Handlingar*, **189**, Goteborg, Sweden, 1–82.

Goenka, P. K. (1984) Analytical Curve Fits for Solution Parameters of Dynamically Loaded Journal Bearings, *Journal of Lubrication Technology*, **106**, 421–428.

Gumbel, L. (1914) Monatsblätter Berliner Bezirksver, *VDI*, **5**, 87–104.

Jakobsson, B. and Floberg, L. (1957) The Finite Journal Bearing Considering Vaporization, *Chalmers Tekniska Hogskolas Handlingar*, **190**, Goteborg, Sweden, 1–116.

Olsson, K. O. (1965) Cavitation in Dynamically Loaded Bearings, *Chalmers Tekniska Hogskolas Handlingar*, **308**, Goteborg, Sweden, 1–60.

Pinkus, O. and Sternlicht, B. (1961) *Theory of Hydrodynamic Lubrication*, McGraw-Hill Book Company, Inc.

Stieber, W. (1933) Das Schwimmlager, *VDI.*, Berlin.

Swift, H. W. (1932) The Stability of Lubricating Film in Journal Bearings, *Proceedings Institute Civil Engineers* (*London*), **233**, 267–288.

Sommerfeld, A. (1904) Zur Hydrodynamischen theorie der Schmiermittelreibung, *Z. Angew. Math. Phys.*, **50**, 97–155.

Vijayaraghavan, D. (1989) Development and Evaluation of a Cavitation Algorithm, *STLE Tribology Transactions*, **32**, 225–233.

Woods, C. M. and Brewe, D. E. (1989) The Solution of the Elrod Algorithm for a Dynamically Loaded Journal Bearing Using Multigrid Techniques, *ASME Journal of Tribology*, **111**, 302–308.

Yu, B. (1999) Lubrication Analysis in the Design of Reciprocating Machinery, *Doctoral Dissertation*, Cleveland State University, Fenn College of Engineering, Cleveland, Ohio.